ADVANCED ELECTRONIC MATERIALS

Supporting Information

for *Adv. Electron. Mater.,* DOI: 10.1002/aelm.201600073

Conquering the Low-*k* Death Curve: Insulating Boron Carbide Dielectrics with Superior Mechanical Properties

*Bradley J. Nordell, Thuong D. Nguyen, Christopher L. Keck, Shailesh Dhungana, Anthony N. Caruso, William A. Lanford, John T. Gaskins, Patrick E. Hopkins, Devin R. Merrill, David C. Johnson, Liza L. Ross, Patrick Henry, Sean W. King, and Michelle M. Paquette**

DOI: 10.1002/aelm.201600073

Supporting Information

Conquering the Low-*k* Death Curve: Insulating Boron Carbide Dielectrics with Superior Mechanical Properties

By *Bradley J. Nordell*, *Thuong D. Nguyen*, *Christopher L. Keck*, *Shailesh Dhungana*, *A. N. Caruso*, *William A. Lanford*, *John T. Gaskins*, *Patrick E. Hopkins*, *Devin R. Merrill*, *David C. Johnson, Liza L. Ross, Patrick Henry, Sean W. King,* and *Michelle M. Paquette**

Prof. M. M. Paquette, B. J. Nordell, T. D. Nguyen, C. L. Keck, S. Dhungana, Prof. A. N. Caruso
Department of Physics and Astronomy
University of Missouri-Kansas City
Kansas City, MO 64110, USA
E-mail: paquettem@umkc.edu

Prof. W. A. Lanford
Department of Physics
University at Albany
Albany, NY 12222, USA

Dr. J. T. Gaskins, Prof. P. E. Hopkins
Department of Mechanical and Aerospace Engineering
University of Virginia
Charlottesville, VA 22904, USA

Dr. D. R. Merrill, Prof. D. C. Johnson
Department of Chemistry and Materials Science Institute
University of Oregon
Eugene, OR 97403, USA

L. L. Ross, Dr. P. Henry, Dr. S. W. King
Logic Technology Development
Intel Corporation
Hillsboro, OR 97124, USA

Table S1. Process parameters and properties of a-BC:H films grown by plasma-enhanced chemical vapor deposition.

Film no.	Temp [°C]	Power [W]	Pressure [Torr]	Total Flow [sccm]	Partial Flow	d [nm]	Growth rate [nm/min]	B/C	At.% O	At.% H	Density [g/cm^3]	E [GPa]	H [GPa]	ε_1	k	$k - \varepsilon_1$	ρ [Ω·cm]	J @ 2 MV/cm [A/cm^2]
Q3	400	40	0.2	100	0.5	169	14.1	3.8	0	15	2.09	323 (±11)	34.7 (±0.8)	6.5	6.7	0.2	4×10^{12}	8×10^{-7}
Q6	400	10	0.2	100	0.1	626	52.2	4.7	4.6	35	1.53	–	–	3.4	3.5	0.1	6×10^{15}	4×10^{-6}
Q7	400	10	0.4	100	0.1	498	41.5	4.4	2.7	35	1.32	–	–	3.7	3.9	0.2	2×10^{14}	4×10^{-7}
Q8	400	10	0.4	50	0.5	722	60.2	4.1	3.9	36	1.40	–	–	3.4	4.2	0.8	6×10^{15}	1×10^{-6}
Q10	400	10	0.4	100	0.9	598	49.8	4.4	3.6	35	1.54	–	–	3.8	4.2	0.4	1×10^{14}	8×10^{-8}
Q11	400	10	0.4	100	1	844	70.3	4.9	4.0	37	1.51	–	–	3.4	4.0	0.6	4×10^{15}	2×10^{-7}
Q12	400	10	0.4	10	1	374	31.2	4.3	2.4	32	1.25	–	–	3.3	4.4	1.1	4×10^{13}	2×10^{-6}
Q15	400	10	0.4	100	0.9	770	64.2	4.3	3.9	36	1.27	–	–	3.3	4.8	1.5	1×10^{16}	2×10^{-7}
Q17	250	10	0.4	200	1	726	60.5	4.7	4.6	35	1.41	–	–	3.7	4.2	0.5	1×10^{14}	3×10^{-8}
Q18	300	10	0.5	100	0.9	388	32.3	4.1	3.4	39	1.32	–	–	3.3	3.9	0.6	5×10^{14}	2×10^{-7}
Q20	400	10	0.4	100	1	1012	84.3	–	–	–	–	–	–	3.4	4.0	0.6	–	–
Q24	400	10	0.4	200	1	837	69.8	4.4	3.8	37	1.27	–	–	3.1	4.0	0.9	1×10^{13}	1×10^{-6}
Q25	400	10	0.4	200	2	1141	95.1	4.5	2.0	37	1.27	–	–	3.3	3.8	0.5	5×10^{13}	[b]
Q27	125	10	0.4	200	2	842	70.2	4.4	3.3	41	1.08	9.8 (±0.5)	0.57 (±0.02)	2.8	3.8	1.0	7×10^{12}	[b]
Q28	75	10	0.4	200	2	192	16.0	3.5	5.4	42	0.94	9 (±1)	0.89 (±0.05)	2.7	3.1	0.4	5×10^{12}	[b]
Q29	275	10	0.4	200	2	396	33.0	4.3	2.4	41	1.30	–	–	3.2	3.6	0.4	1×10^{13}	1×10^{-7}
Q30	400	10	0.4	50	1	379	31.5	4.2	2.1	34	1.46	–	–	3.6	4.5	0.9	6×10^{15}	[b]
Q33	250	10	0.4	100	1	152	12.7	–	–	–	–	–	–	2.9	3.2	0.3	1×10^{14}	2×10^{-7}
Q34[a]	250	10	0.4	200	2	845	70.4	–	–	–	–	–	–	3.0	–	–	–	–
Q35[a]	250	10	0.4	200	1	–	–	–	–	–	–	–	–	–	–	–	–	–
Q37	250	10	0.4	10	1	153	12.8	–	–	–	–	–	–	2.8	3.7	0.9	1×10^{14}	1×10^{-7}
Q40	250	10	0.4	20	2	299	24.9	–	–	–	–	–	–	2.8	3.5	0.7	5×10^{13}	5×10^{-7}
Q4	250	40	2	300	0.3	97	8.1	4.0	4.7	37	1.50	–	–	3.3	3.9	0.6	2×10^{14}	1×10^{-7}
Q5	200	40	2	200	0.5	47	3.9	4.7	4.9	34	1.60	–	–	3.1	3.7	0.6	5×10^{13}	2×10^{-7}
Q13	200	40	2	100	1	45	3.8	–	–	–	–	–	–	3.0	3.3	0.3	9×10^{12}	5×10^{-7}
Q14	250	40	2	100	1	60	5.0	4.1	6.0	32	1.63	34 (±2)	4.1 (±0.3)	3.5	3.7	0.2	4×10^{13}	8×10^{-8}
Q16	200	40	2	200	1	66	5.5	2.9	7.5	33	1.23	–	–	3.2	3.4	0.2	3×10^{14}	1×10^{-7}
Q19	300	40	2	100	1	51	4.3	–	–	–	–	–	–	3.0	2.8	N/A	2×10^{11}	1×10^{-5}
Q26	400	40	2	200	2	92	7.7	3.3	5.9	30	1.51	96 (±5)	10.6 (±0.3)	3.6	3.9	0.3	2×10^{13}	1×10^{-7}
Q31	125	40	2	200	2	55	4.6	–	–	–	–	–	–	2.6	2.9	0.3	6×10^{12}	2×10^{-5}
Q32a	275	40	2	200	2	200	16.7	5.1	7.8	34	1.50	126 (±5)	8.6 (±0.4)	2.7	3.0	0.3	1×10^{15}	1×10^{-8}
Q32b	275	40	2	200	2	189	15.8	4.2	3.1	41	1.37	–	–	3.1	3.4	0.3	3×10^{14}	2×10^{-8}
Q36	250	40	8	200	2	164	13.7	–	–	–	–	–	–	2.8	3.2	0.4	2×10^{13}	2×10^{-7}
Q42	150	40	2	200	2	67	5.6	–	–	–	–	–	–	2.4	2.6	0.2	5×10^{11}	[b]
Q43	600	40	2	200	2	504	42.0	–	–	–	–	202 (±9)	17 (±1)	4.6	5.5	0.9	3×10^{12}	[b]
Q45	375	40	2	200	2	100	8.3	4.3	6.8	39	1.20	–	–	3.3	3.7	0.4	2×10^{14}	7×10^{-9}

[a]Delaminated. [b]Electrical breakdown occurred at <2MV/cm.

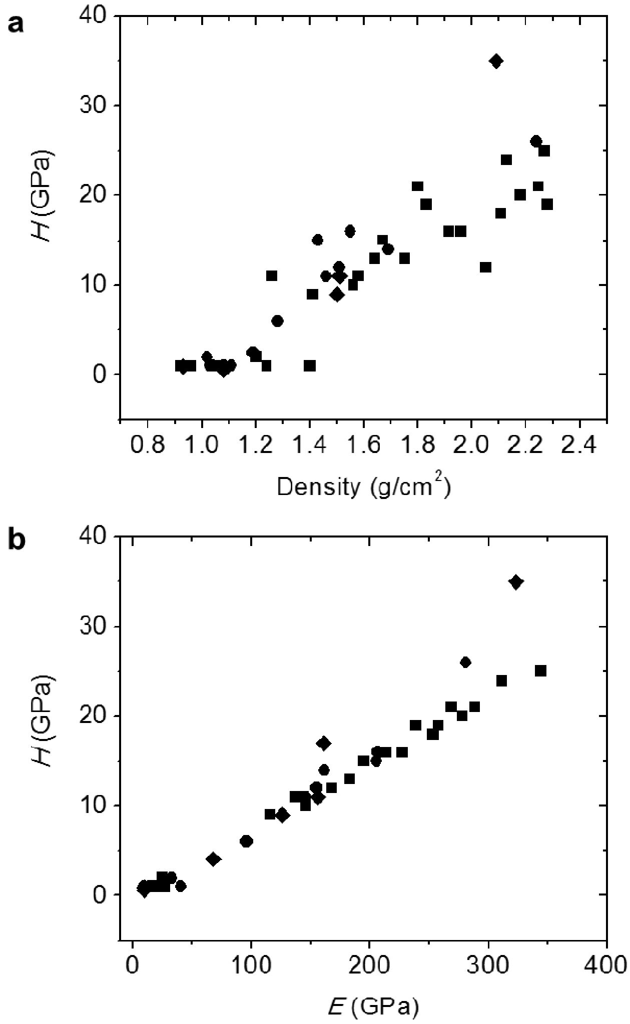

Figure S1. Mechanical properties of a-BC:H films. (a) Hardness vs density. (b) Hardness vs Young's modulus (■ = ref[1], ● = ref[2], ◆ = this work).

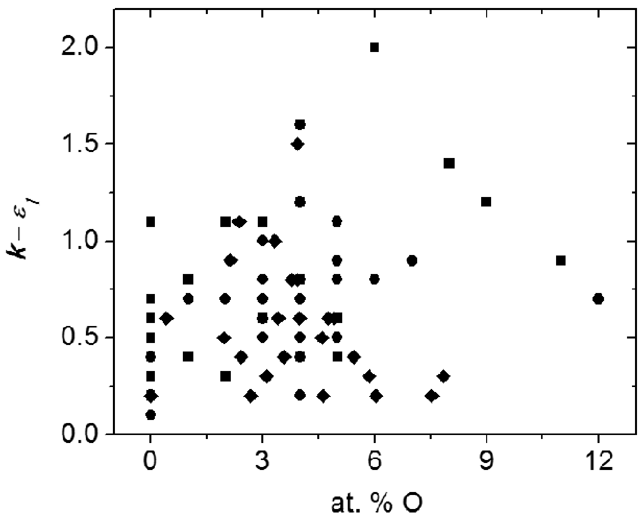

Figure S2. Scatter plot illustrating lack of correlation between ionic/orientation polarization term ($k - \varepsilon_1$) and oxygen concentration.

Table S2. Reproducibility of dielectric and electrical properties in a-BC:H film **A** (Q32/DB1).

Film	Thickness [nm]	ε_1	k	$k - \varepsilon_1$	J [A/cm^2] (0.5 MV/cm)	J [A/cm^2] (2 MV/cm)
Q32a	200	2.7	3.0	0.3	1×10^{-10}	1×10^{-8}
Q32b	189	3.1	3.4	0.3	5×10^{-10}	2×10^{-8}
Q32c	52	3.1	3.3	0.2	5×10^{-10}	8×10^{-9}
Q32d	50	3.1	–	–	1×10^{-10}	1×10^{-8}
Q32e.1	22	3.0	Too thin	–	7×10^{-10}	3×10^{-9}
Q32e.9	36	3.0	Too thin	–	7×10^{-10}	5×10^{-9}
Q32f	65	3.0	3.3	0.3	8×10^{-10}	8×10^{-9}
Q32k	22	2.8	Too thin	–	4×10^{-10}	2×10^{-9}
DB1a	150	3.1	3.4	0.3	5×10^{-10}	2×10^{-8}
DB1b	3.5	2.8	Too thin	–	5×10^{-10}	5×10^{-9}
DB1c	121	3.1	–	–	3×10^{-10}	1×10^{-8}
Average		3.0 ± 0.14	3.3 ± 0.15	0.3 ± 0.04	4.6×10^{-10} ($\pm 2.2 \times 10^{-10}$)	9.2×10^{-9} ($\pm 5.7 \times 10^{-9}$)

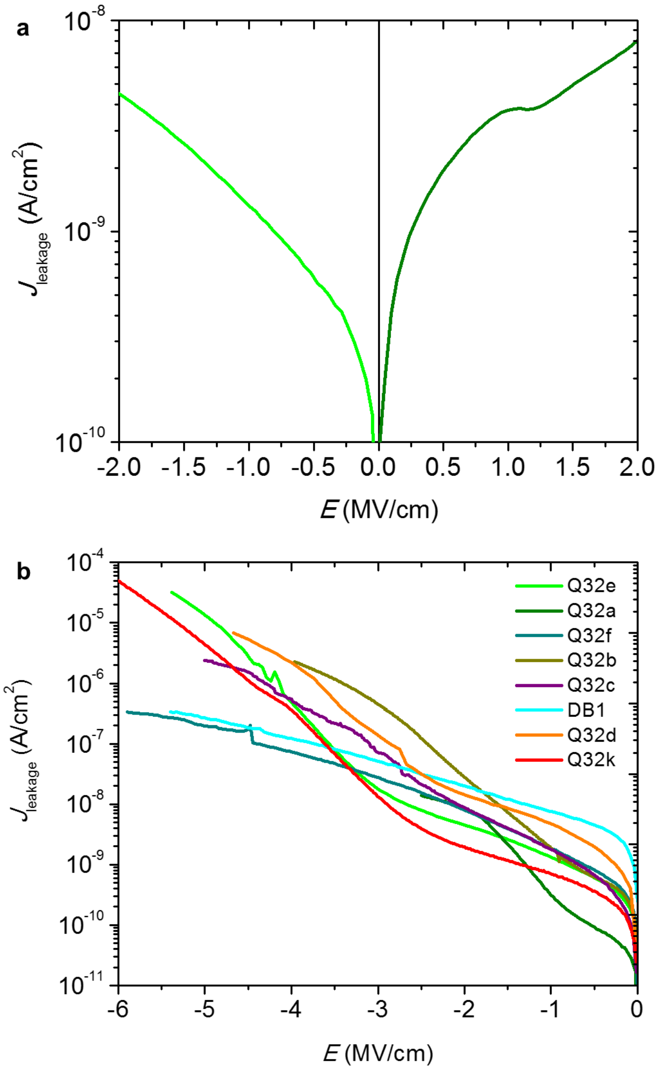

Figure S3. Leakage current curves of a-BC:H film **A**. (a) Symmetry of current density at forward and reverse biases. (b) reproducibility of *JE* curves for various Q32 samples. In many cases, the maximum electric field was limited to an applied voltage of 200 V.

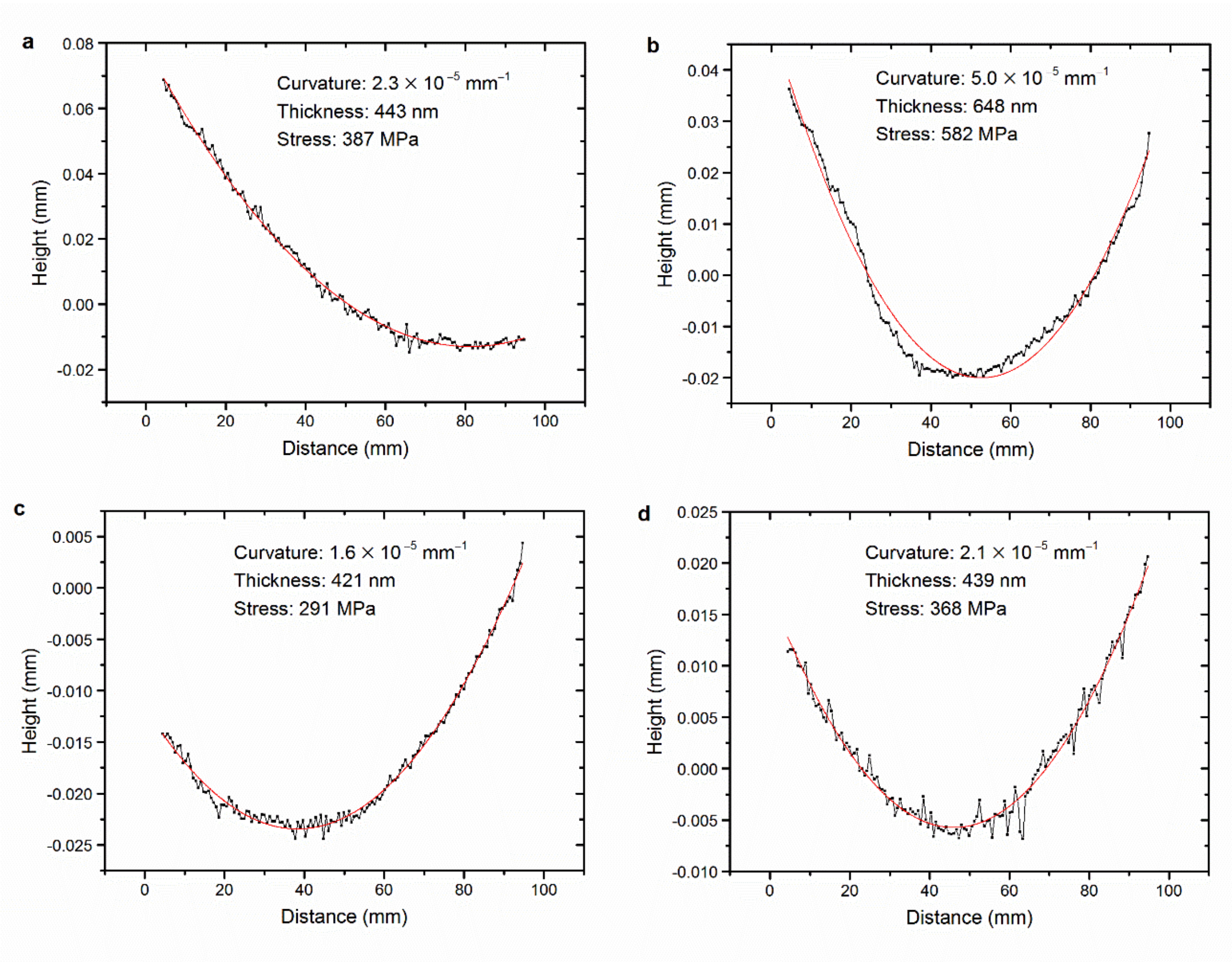

Figure S4. Optical profilometry data for four independently grown a-BC:H **A** samples after subtracting the background for the silicon substrate, from which film stress was extracted based on the wafer curvature method.

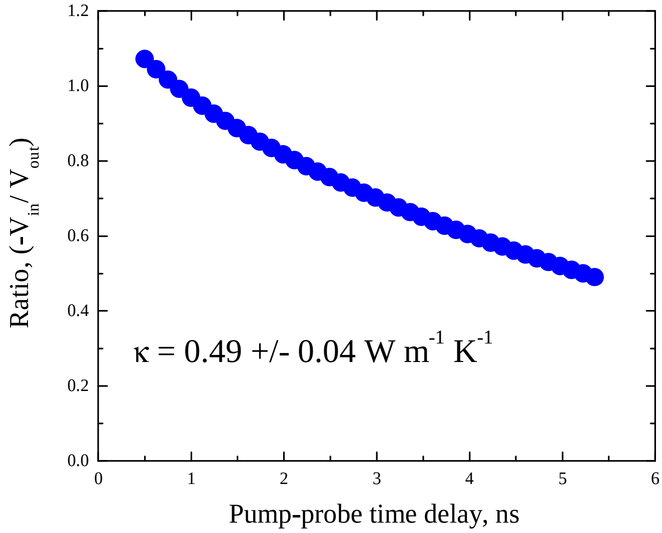

Figure S5. Averaged data from five time domain thermoreflectance (TDTR) scans at discrete locations on a sample of a-BC:H **A** (Q32b) yielding a thermal conductivity of 0.49 ± 0.04 W•m^{-1}•K^{-1}. The TDTR experiment uses a high-energy, high-repetition-rate laser beam to excite a thermal event on an aluminum film and a co-linear low-energy beam to monitor the changes in reflectivity of the same aluminum film. These changes over time can then be related back to the thermophysical properties of the underlying layers. Error values are largely due to uncertainty in the thickness of the aluminum transducer and not from test to test repeatability. It should be noted that the fit to the data and standard deviation are smaller than the data points. More information on the analysis can be found elsewhere.[3–5]

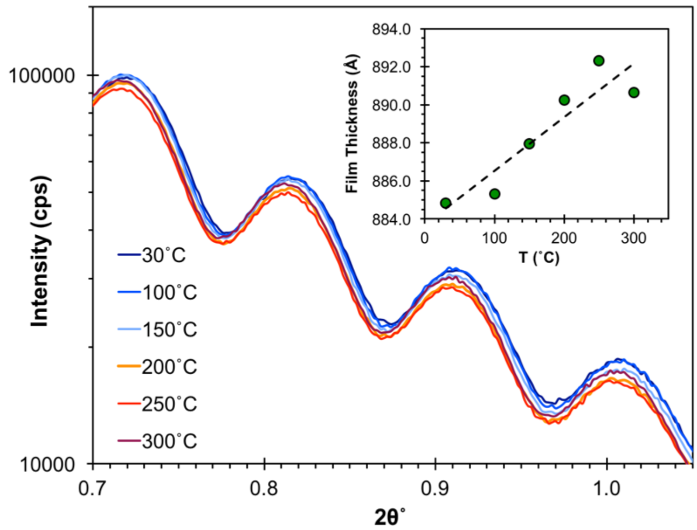

Figure S6. Overlay of raw X-ray reflectivity data given as a function of temperature. The modeled thicknesses are shown in the inset. The large roughness of the film lowers the certainty in the slope, resulting in the large uncertainty in the reported value.

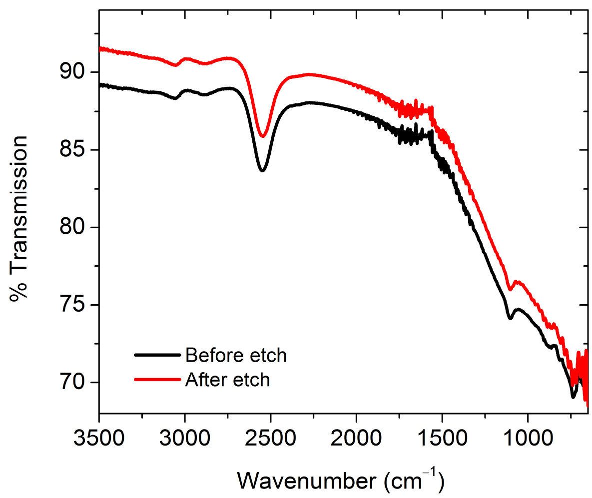

Figure S7. FTIR spectrum for a moderate-density a-BC:H film before and after 10 min immersion in 1% KOH solution.

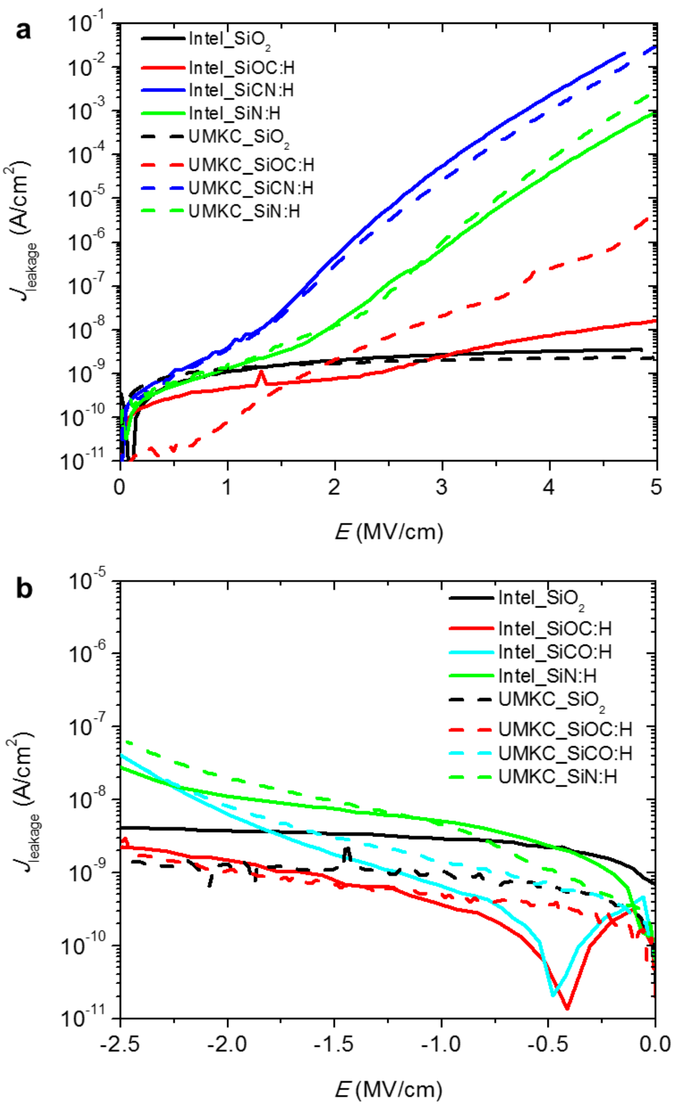

Figure S8. Comparison of Hg probe leakage current measurements from independent tools at Intel and UMKC for a series of low-*k* dielectric standard films with thicknesses of (a) 200 nm and (b) 500 nm.

Table S3. Comparison of Hg probe measurements of leakage current (From Figure S8) and dielectric constant (*k*) using independent tools at Intel and UMKC for a series of low-*k* dielectric standards with thicknesses of 200 or 500 nm.

	J **[A/cm²] (2 MV/cm) (200 nm, Intel)**	***J*** **[A/cm²] (2 MV/cm) (200 nm, UMKC)**	***J*** **[A/cm²] (2 MV/cm) (500 nm, Intel)**	***J*** **[A/cm²] (2 MV/cm) (500 nm, UMKC)**	***k*** **(500 nm, Intel)**	***k*** **(500 nm, UMKC)[a)]**
SiO_2	2×10^{-9}	2×10^{-9}	4×10^{-9}	1×10^{-9}	4.37	4.41 (±0.25)
SiCN:H	5×10^{-7}	3×10^{-7}	–	–	5.93	5.99 (±0.27)
SiCO:H	–	–	6×10^{-9}	8×10^{-9}	4.70	4.68 (±0.21)
SiN:H	1×10^{-8}	1×10^{-8}	1×10^{-8}	2×10^{-8}	6.79	6.63 (±0.25)
SiOC:H	8×10^{-10}	2×10^{-9}	2×10^{-9}	1×10^{-9}	3.01	2.97 (±0.21)

[a)]Reported as the average of 6–10 measurements

[1] B. J. Nordell, S. Karki, T. D. Nguyen, P. Rulis, A. N. Caruso, S. S. Purohit, H. Li, S. W. King, D. Dutta, D. Gidley, W. A. Lanford, M. M. Paquette, *J. Appl. Phys.* **2015**, *118*, 035703.

[2] B. J. Nordell, C. L. Keck, T. D. Nguyen, A. N. Caruso, S. S. Purohit, W. A. Lanford, D. Dutta, D. Gidley, P. Henry, S. W. King, M. M. Paquette, *Mater. Chem. Phys.* **2016**, *173*, 268.

[3] D. G. Cahill, *Rev. Sci. Instrum.* **2004**, *75*, 5119.

[4] A. J. Schmidt, X. Chen, G. Chen, *Rev. Sci. Instrum.* **2008**, *79*, 114902.

[5] P. E. Hopkins, J. R. Serrano, L. M. Phinney, S. P. Kearney, T. W. Grasser, C. T. Harris, *J. Heat Transfer* **2010**, *132*, 081302.